Plant Physiology, February 1999, Vol. 119, pp. 681–692, www.plantphysiol.org © 1999 American Society of Plant Physiologists

Regulation of Growth Anisotropy in Well-Watered and Water-Stressed Maize Roots. II. Role of Cortical Microtubules and Cellulose Microfibrils[1]

Tobias I. Baskin*, Herman T.H.M. Meekes, Benjamin M. Liang, and Robert E. Sharp

Division of Biological Sciences (T.I.B., H.T.H.M.M.) and Department of Agronomy, Plant Science Unit (B.M.L., R.E.S.), University of Missouri, Columbia, Missouri, 65211

We tested the hypothesis that the degree of anisotropic expansion of plant tissues is controlled by the degree of alignment of cortical microtubules or cellulose microfibrils. Previously, for the primary root of maize (*Zea mays* L.), we quantified spatial profiles of expansion rate in length, radius, and circumference and the degree of growth anisotropy separately for the stele and cortex, as roots became thinner with time from germination or in response to low water potential (B.M. Liang, A.M. Dennings, R.E. Sharp, T.I. Baskin [1997] Plant Physiol 115:101–111). Here, for the same material, we quantified microtubule alignment with indirect immunofluorescence microscopy and microfibril alignment throughout the cell wall with polarized-light microscopy and from the innermost cell wall layer with electron microscopy. Throughout much of the growth zone, mean orientations of microtubules and microfibrils were transverse, consistent with their parallel alignment specifying the direction of maximal expansion rate (i.e. elongation). However, where microtubule alignment became helical, microfibrils often made helices of opposite handedness, showing that parallelism between these elements was not required for helical orientations. Finally, contrary to the hypothesis, the degree of growth anisotropy was not correlated with the degree of alignment of either microtubules or microfibrils. The mechanisms plants use to specify radial and tangential expansion rates remain uncharacterized.

During animal morphogenesis, cells grow, move, contract, or die, whereas in plant morphogenesis, cells only grow. A growing plant organ, to produce any other form than a sphere, must grow at different rates in different locations or directions. When growth rates are different and in different directions, growth is said to be anisotropic. Anisotropy is a nearly ubiquitous feature of plant growth, not only for the leaves of grasses and cylindrical organs such as coleoptiles, stems, and roots, which expand principally in length, but also for laminar organs such as dicot leaves and petals, which may expand isotropically in the plane of the lamina but which expand minimally perpendicularly to the lamina. Growth anisotropy has even been reported for tip-growing cells in the rare cases in which both axial and tangential growth components have been resolved (Castle, 1958; Green, 1965).

Plants control expansion by controlling how the cell wall yields to turgor pressure. Because turgor pressure is isotropic, the cell wall can yield anisotropically only when the mechanical properties of the cell wall are anisotropic. The most prominent anisotropic component of the cell wall is cellulose. This polymer is synthesized at the plasma membrane as long chains of β-1,4-linked glucose residues that associate laterally into microfibrils (Brown et al., 1996). Microfibrils are usually aligned in parallel, which reinforces the cell wall anisotropically and may guide the subsequent assembly of polymers around the cellulose framework (Cosgrove, 1997). In the diffusely growing cells of higher plants, the aligned deposition of microfibrils is thought to be dictated by the alignment of cortical microtubules (Cyr, 1994; Wymer and Lloyd, 1996).

Anisotropic expansion is characterized by two parameters: the direction in which the maximal expansion rate occurs and the degree to which the maximal expansion rate exceeds the minimal rate. The direction of maximal expansion is specified by the direction of the cellulose microfibrils, according to several lines of evidence. First, the axis of maximal expansion rate is usually perpendicular to the net alignment of microfibrils (Green, 1980; Taiz, 1984). Second, growth anisotropy is reduced or even eliminated when microfibril synthesis is inhibited chemically or genetically (Hogetsu et al., 1974; Arioli et al., 1998). Third, expansion becomes essentially isotropic when, during development or in response to inhibitors or hormones, microfibrils are deposited without a predominant alignment (Richmond, 1983; Hogetsu, 1989; Iwata and Hogetsu, 1989; Sakaguchi et al., 1990). Finally, cell cultures can be obtained that have scant cellulose in their cell walls and that undergo turgor-driven enlargement (Shedletzky et al., 1990) but, to our knowledge, these never expand anisotropically.

In contrast to the direction of maximal expansion rate, there is almost no information about what controls the degree of anisotropy. One reason for this lack is that radial or tangential expansion rates are rarely quantified and so

[1] This paper is dedicated to the memory of Paul B. Green (1931–1998). This project was funded in part by grant no. 94ER20146 (to T.I.B.) from the U.S. Department of Energy and does not constitute endorsement by that department of views expressed herein by the University of Missouri Research Board (award no. RB-95038 to T.I.B.), by the Cooperative States Research Service, U.S. Department of Agriculture (award no. 95-37100-1601 (with R.E.S. and W.G. Spollen), and by the University of Missouri Food for the 21st Century Program (R.E.S). This is a contribution from the Missouri Agricultural Experiment Station, journal series no. 12,841.

* Corresponding author; e-mail baskin@biosci.mbp.missouri.edu; fax 1–573–882–0123.

the degree of growth anisotropy is usually unknown. An exception is the giant internode of characean algae, for which the ratio of growth rate in length to diameter is about 4.5 (Green, 1964). However, this ratio remains constant during development, so that the studies of the role of cellulose microfibrils in the control of expansion using these cells have not provided insight about variation in the degree of growth anisotropy (Taiz, 1984).

There is a further difficulty that has limited our understanding of how the degree of growth anisotropy is controlled in the organs of higher plants. For a single cell such as an algal internode, growth anisotropy is characterized by the changes in cell length and diameter; however, for a cylindrical, multicellular organ such as a root, measurements of elongation and organ diameter over time are not sufficient. Although all tissues at a given distance from the apex must elongate at the same rate (otherwise the root would tear or cells would slip), different tissues, e.g. the stele and cortex, may expand in diameter at different rates. Moreover, expansion in diameter has two components, radial and tangential (i.e. circumferential), and these do not have to be equal at a given location (Liang et al., 1997). Therefore, the degree of growth anisotropy may differ between different tissues as well as between cell walls in tangential and radial planes.

To our knowledge, the only study to have measured rates of expansion in diameter separately for different tissues and to obtain both radial and tangential terms is the first paper in this series, concerning the control of growth anisotropy in the primary root of maize (*Zea mays*) (Liang et al., 1997). These roots become thinner with time from germination, reaching steady-state growth after about 3 d. We found for both the cortex and stele that neither radial nor tangential expansion rate was proportional to elongation rate and, hence, unlike the giant algal internodes, the degree of growth anisotropy varied. In fact, the degree of anisotropy, calculated as the ratio of longitudinal to radial (or to tangential) expansion rate varied with time and between positions by more than 1 order of magnitude. Additionally, we analyzed directional expansion rates in roots exposed to a water-stress treatment, which had been previously shown to cause the roots to thin (Sharp et al., 1988). The reduced diameter contributes significantly to the maintenance of root elongation under water stress because root volume decreases as the square of the radius and hence less water and solutes are needed for growth (Sharp et al., 1990). The degree of growth anisotropy in water-stressed roots differed markedly from well-watered roots, being increased in the apical region of the growth zone and decreased in the basal region.

As an approach to understanding what determines the spatial profiles of expansion rate and anisotropy, the objective of this study was to quantify the alignments of microtubules and microfibrils as a function of position in both well-watered and water-stressed roots. Our results bear on three related questions. First, what is the relationship between the alignments of microtubules and microfibrils? These alignments have been compared most often in the epidermis of stems; however, in this tissue comparisons are hindered by the orientations continually shifting among transverse, longitudinal, and oblique. Second, is elongation rate controlled by the alignments of microtubules or microfibrils? Because both are generally observed to be transverse during rapid elongation and oblique (or longitudinal) otherwise, the alignment of these elements has been suggested to control elongation rate. Third, what controls the degree of growth anisotropy? The answer has been hypothesized to be the degree of alignment among cellulose microfibrils, but this hypothesis has not been tested decisively. Answering this question is essential because until we know how cells expand anisotropically, we will not understand plant morphogenesis.

MATERIALS AND METHODS

Seeds of maize (*Zea mays* L. cv FR27 × FRMo17) were germinated, then transplanted into vermiculite at a water potential of approximately −0.03 MPa (well-watered) or approximately −1.63 ± 0.08 MPa (water-stressed, mean ± SD, $n = 20$; water potential was measured in every experiment), and grown in darkness at 29°C and near-saturation humidity, as described by Liang et al. (1997). Well-watered roots were harvested at 24 or 48 h and water-stressed roots were harvested 48 h after transplanting. Primary roots used for all results reported here were selected to be elongating within ±10% of the mean rate (approximately 3 mm h^{-1} for well-watered and 1 mm h^{-1} for water-stressed roots).

Microtubule Localization

The protocol for immunocytochemical localization of microtubules was described by Liang et al. (1996). Apical 20-mm root segments were fixed for 1.5 h in 50 mM Pipes buffer containing 4% paraformaldehyde, sectioned longitudinally at 100-μm thickness on a Vibratome (V-1000, Technical Products International, St. Louis, MO), collected on slides, and incubated successively in primary (mouse monoclonal against chicken brain β-tubulin, Amersham) and secondary (Cy3-conjugated goat anti-mouse IgG, Jackson ImmunoResearch Laboratories, West Grove, PA) antibodies. For qualitative assessment, sections were peeled off the slide, leaving cortical cytoplasm affixed to the slide (Liang et al., 1996). Such preparations will be referred to as microtubule peels. Quantification was done on sections to avoid the potential for the peeling process to alter microtubule angles. To assay the sensitivity of cortical arrays to cold-induced depolymerization, seedlings were put into thin plastic bags (to prevent water uptake) and submerged in ice water (0°C) in a vertical position for 0, 3, 6, or 10 min, and then were fixed and processed as described above. Preliminary experiments showed that cortical arrays were not visibly affected when roots were placed in plastic bags and immersed in water at 29°C for 10 min.

To quantify microtubule angles, we selected from each root a single longitudinal section near the median. Images made with conventional epifluorescence microscopy were captured digitally at 0.5-mm increments along the root, with the boundary between the root cap and quiescent center, which was visible in all sections, used as a common origin. Microtubule angular distributions were measured

with an image-analysis program (Image 1, Universal Imaging, West Chester, PA).

Polarized-Light Microscopy

Apical 6-mm segments were fixed in 50 mM Pipes buffer containing 1 mM $CaCl_2$ and 4% paraformaldehyde at room temperature for 2 h. After the segments were rinsed, they were embedded in butyl-methyl-methacrylate, as described by Baskin and Wilson (1997), except that wire loops were not used because of the large size of the root. The methacrylate's refractive index (n = 1.533, Bayley et al., 1957) matches that of cellulose and other polysaccharides and thus suppresses "form birefringence," which results from the alignment of polymers of one refractive index within a medium of another (Preston, 1974). Sections (2 μm thick) were spread with chloroform vapor and baked on silane-coated slides for several hours. Measurements of the length of the root segment before fixation and after embedding showed negligible shrinkage, as previously found for this type of methacrylate (Carlemalm et al., 1982); however, sectioning shortened the length of the root segment by about 10%, which was not corrected for in the ordinate of Figure 7.

Sections were mounted in a 75% glycerol, 0.01% Triton X-100 solution and examined through a polarized-light microscope equipped for microphotometry (Jenapol, Zeiss). Longitudinal-radial cell walls that were contained in the plane of approximately median-longitudinal sections were examined. The stage was rotated to place the cell walls at extinction and then rotated by 45°. A suitable cell wall was translated to the optical axis, where a small square aperture (15 μm^2 at the magnification used) reflected 100% of the light to a photomultiplier with a digital read-out of intensity. Intensities were measured for ±45° settings of the compensator (Brace-Köhler type, Γ_{max} = 18 nm). An adjacent background area outside the root was then translated to the optical axis, and the intensity was measured at ±45° compensator settings. At every 0.5 mm from the boundary between the root cap and quiescent center, cell walls were measured that were no more than 50 μm from the defined position.

Retardation was calculated from the intensity measurements with the compensator equations (Jerrard, 1948) as follows. The intensity through a single birefringent plate at 45° between crossed polars (i.e. through the background), I_b, is given by:

$$I_b = I_o \sin^2\left(\frac{\delta_1}{2}\right) \quad (1)$$

where I_o is the incident light intensity and δ_1 is the maximal retardation of the compensator (18 nm). The intensity through two birefringent plates at ±45° between crossed polars (i.e. through the cell wall), I_w, is given by:

$$I_w = I_o\left(\sin^2\frac{\delta_1}{2}\cos\delta_2 \pm \frac{1}{2}\sin\delta_1 \sin\delta_2 + \sin^2\frac{\delta_2}{2}\right) \quad (2)$$

where δ_2 is the retardation of the specimen, and the sign of the second term is given by the sign of the compensator (i.e. ±45°). The specimen retardation was then obtained by simultaneous solution of the equations. For convenience, Equation 2 was simplified by using the small angle approximation ($\cos x = 1$; $\sin x = x$) for δ_2. This assumption was validated by finding that the error from the small angle approximation was less than the precision of the photomultiplier. The values from the two compensator settings were averaged to produce a single datum point for each measured cell wall.

Replicas of Cellulose Microfibrils

Apical 20-mm root segments were fixed in 4% paraformaldehyde in deionized water for 30 min, rinsed in water several times, and sectioned on the Vibratome as described above. From each root three approximately median sections were placed in a 20-mL vial and rinsed in distilled water for at least 2 h. Sections were then incubated in 0.5 M Na_2CO_3 at room temperature for 3 d to remove pectin, with several changes of the solution. After two to three rinses in double-distilled water, the sections were placed on nitrocellulose sheets clamped on microscope slides and allowed to dry overnight at 30°C. The preparations were shadowed at an acute angle with platinum, and subsequently from above with carbon, in a vacuum evaporator (DV 502, Denton, St Louis, MO). Under a stereomicroscope, the shadowed sections were cut into 0.5-mm segments starting at the line between root cap and quiescent center. Segments originating from the same positions along different roots within the same experiment and treatment were pooled. To release the nitrocellulose and remove tissue remnants, segments were treated with 25% Cr_2O_3 solution for at least 4 h and then with dilute bleach (about 0.25%) for 1 h. After the replicas were rinsed extensively, they were mounted on 60-mesh hexagonal copper grids and viewed in an electron microscope (model 1200, JEOL).

Replicas of longitudinal-radial cell walls of cortical cells were photographed at ×25,000, with the orientation indicated by including a transected longitudinal cell wall. Images of the microfibrils were projected through a photographic enlarger onto a circle with a diameter at the level of the cell of 600 nm. Each microfibril was traced at the circumference of the circle, and the angle of the traces with respect to the root axis was measured using a digitizing tablet and software (SigmaScan, Jandel Scientific, Corte Madera, CA). For measurement, the longitudinal axis was defined as 0° and 180°. To average microfibril angles meaningfully, the definition of zero was moved in 1° increments through a total of 180° by addition or subtraction of 180° to appropriate subsets of the data; for each increment, a mean ± SD was calculated and the lowest SD was used to select the best average, which was then transformed back to its original angle with respect to the longitudinal axis.

To view microtubules and cellulose microfibrils in the same sections, microtubule peels were prepared from median longitudinal sections as described above, and after peeling, the sections were processed for microfibril replicas. To ensure that the replicas were made from the same side of the section from which the microtubule peel had been made, the two sides of the section were identified by

cutting the basal end of the section obliquely. Care was taken to account for all inversions of the image during electron microscopy by the use of asymmetric internal features (e.g. numerals on the grid).

For the growth data obtained previously (Liang et al., 1997), the distal end of the root cap was defined as the apex; therefore, to be consistent, for all distances measured here with respect to the boundary between root cap and quiescent center, we added the average root cap length (about 500 μm for all treatments), which was measured from approximately median longitudinal Vibratome sections of unfixed roots.

RESULTS

Radial Expansion Rates and the Degree of Growth Anisotropy

The first paper in this series (Liang et al., 1997) showed that the spatial profiles of radial and tangential expansion rates in the maize primary root changed in well-watered roots with time from germination ("developmental" thinning) and also changed in roots transplanted to low water potential (−1.6 MPa, "water stress"). The developmental thinning and the thinning induced by water stress resulted from decreased radial and tangential expansion rates in both the cortex and stele. Here we focused on the cortex, although some results were obtained for the stele, because cortical cells are more homogeneous in shape. Also, for the cortex we considered radial rather than tangential expansion rates, because the cell walls expected to limit radial expansion are longitudinal-radial walls, which can be assayed conveniently in median-longitudinal sections. For the stele, tangential and radial expansion rates are assumed to be equal (Liang et al., 1997). We did not analyze the epidermis because this tissue was not reliably retained in the preparations.

To enable the reader to compare readily the spatial profiles of expansion rate with the results presented below for microtubule and microfibril orientation, we reproduce relevant data from Liang et al. (1997) in Figure 1. The developmental thinning of well-watered roots was analyzed by comparing them at 24 and 48 h after transplanting. The profile of longitudinal strain rate (i.e. relative elemental elongation rate) was similar at these times (Fig. 1A). In contrast, radial strain rates in the cortex differed: around 3 mm from the apex, radial strain rates at 48 h were high, whereas those at 24 h were essentially 0, and between 6 and 9 mm from the apex, rates at 48 h decreased to 0, whereas those at 24 h remained high and even increased (Fig. 1B). Accordingly, the degree of growth anisotropy, calculated as the ratio of longitudinal to radial strain rate, was strikingly different at the two times (Fig. 1C). Anisotropy increased with position in the apical 4 mm of the root but reached much higher values at 24 h compared with 48 h; basal of 4 mm, anisotropy decreased steadily at 24 h but at 48 h decreased and then increased steeply.

The effect of low water potential was analyzed by comparing well-watered and water-stressed roots 48 h after transplanting, when growth in both treatments had reached

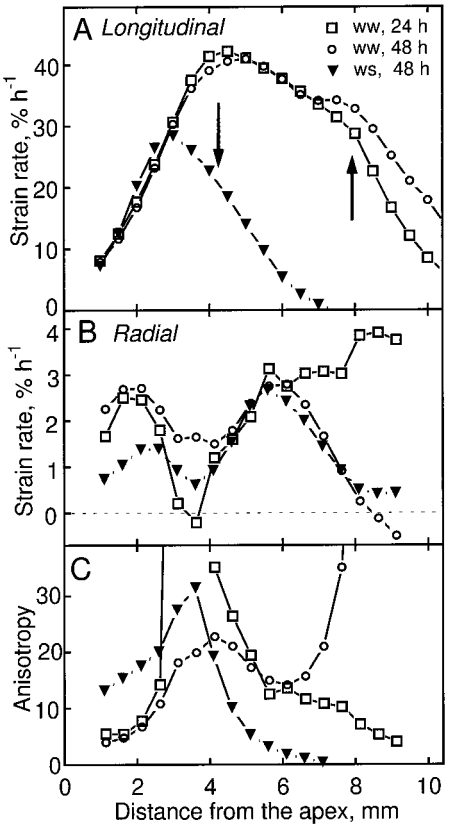

Figure 1. Longitudinal and radial strain rates as a function of distance from the apex for well-watered (ww, 24 and 48 h after transplanting) and water-stressed (ws, 48 h after transplanting) roots. The data are from Liang et al. (1997). A, Longitudinal strain rate. Arrows indicate positions where microtubule orientation changed from transverse to oblique (Fig. 3). B, Radial strain rate for the cortex. C, Growth anisotropy, calculated as the ratio of longitudinal to radial strain rates. Note that when radial strain rates are near 0 growth anisotropy tends toward infinity; these values are not plotted.

steady state (Liang et al., 1997). Longitudinal strain rates were similar in the apical 3 mm of the root, and basal of this they were reduced in the water-stressed roots (Fig. 1A), as previously reported (Sharp et al., 1988). In contrast, radial strain rates in the cortex were decreased in the apical 4 mm of the water-stressed roots but at more basal locations were identical in the two treatments (Fig. 1B). Consequently, the degree of growth anisotropy in the water-stressed roots was substantially higher than in the well-watered roots in the apical 4 mm of the root and basal to this was substantially lower (Fig. 1C). Thus, both the developmental thinning of the roots and the further thinning imposed by water stress changed radial expansion rates and the degree of growth anisotropy appreciably.

Localization of Microtubules

In median-longitudinal sections, cortical microtubule arrays in cortex cells had distinct orientations at defined distances from the apex. Examples are shown of transverse, oblique, and longitudinal orientations for both well-watered

and water-stressed roots (Fig. 2). We reported previously that the appearance of obliquely oriented microtubules in sections or peels reflects the fact that the cortical array forms a helix around the cell; moreover, the handedness of the helix at defined positions was conserved among roots (Liang et al., 1996). With increasing distance from the apex, transverse arrays were replaced by right-handed helices, longitudinal arrays, and then by left-handed helices. This progression was the same for well-watered and water-stressed roots, although as shown below, the positions where the transitions occurred were different between the treatments. Comparing the two treatments, microtubule arrays of the same orientation could not be distinguished visually.

Quantification of Microtubule Orientation

To determine the extent to which microtubule orientation was associated with the profiles of expansion rate, we quantified the angular distribution of microtubules as a function of position. Results for the cortex are shown in Figure 3. The net orientation of microtubules was similar in the 24- and 48-h well-watered roots (Fig. 3A): microtubules were transverse until nearly 8 mm from the apex and then steadily reoriented until they reached a stable orientation of approximately 225° (left-handed helix). For the water-stressed roots, the reorientation of microtubules began and ended nearer to the apex. In both treatments the mean orientation of microtubules was transverse throughout much of the growth zone, which is consistent with the fact that elongation rates were consistently greater than radial expansion rates, i.e. the degree of anisotropy was greater than 1 (Fig. 1).

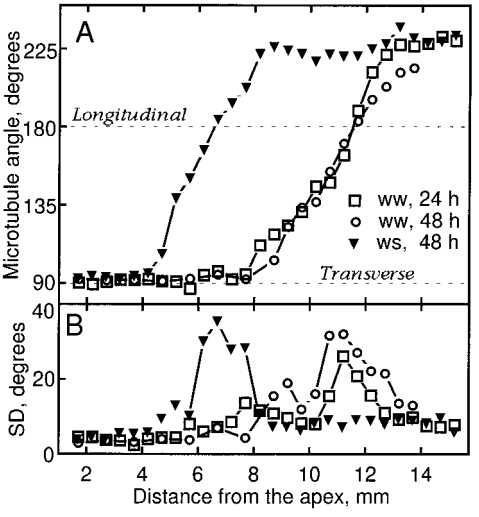

Figure 3. Microtubule orientation in cortical cells as a function of distance from the apex of well-watered (ww) and water-stressed (ws) roots. A, Mean microtubule angle measured for cells localized in median-longitudinal sections. B, The SDs of the above distributions. At each position, 20 microtubules were sampled from two cells, and the data presented were pooled from measurements of 5 to 10 roots (100–200 microtubules measured per position).

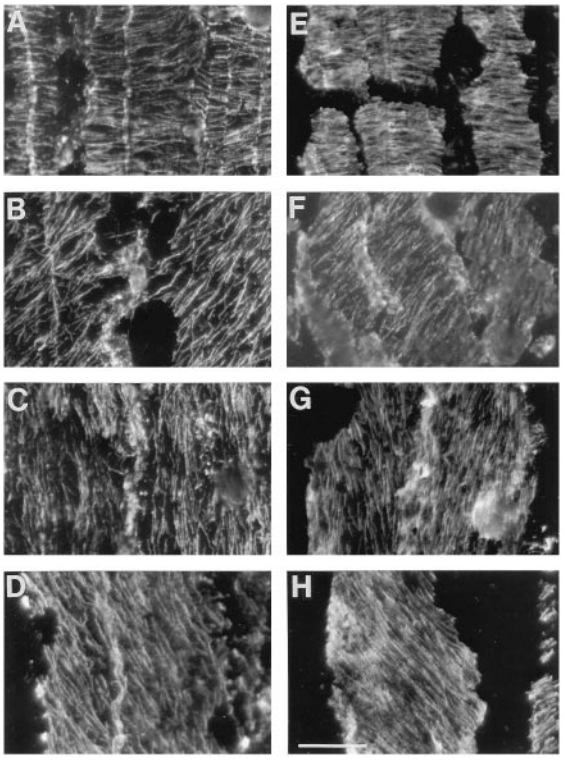

Figure 2. Micrographs of cortical microtubules in median-longitudinal sections showing the similar appearance of transverse, oblique, and longitudinal orientations in cells of the cortex of well-watered and water-stressed roots. A to D, Well-watered roots; E to H, water-stressed roots. Examples of transverse (A and E), oblique (B and F; right-handed helical), longitudinal (C and G) , and oblique (D and H; left-handed helical) microtubule orientations. Micrographs were obtained from peels, as described in "Materials and Methods." Bar = 20 μm.

We compared the standard deviation of microtubule angle to radial strain rates and to the degree of growth anisotropy. In all cases, the deviation among microtubules slowly increased with distance from the apex until mean microtubule orientation was near longitudinal, when the deviations grew notably (Fig. 3B). Once the mean orientation reached the stable oblique orientation (i.e. 225°), the deviations again became smaller. Thus, the degree of microtubule alignment tended to change in parallel with the net orientation of the array but not in relation to the changed spatial profiles of either radial expansion rate or growth anisotropy. For example, between 6 and 9 mm from the apex, the deviation in microtubule orientation was similar for well-watered roots at 24 and 48 h despite the large differences between them in radial expansion rates and the degree of anisotropy (Fig. 1, B and C).

To extend these results, we compared microtubule orientations between well-watered and water-stressed roots in the stele (Fig. 4). The tangential (radial) strain rates were considerably reduced in the apical 5 mm of the water-stressed stele (Fig. 4A), and the spatial profile of the degree of growth anisotropy was quite different between the two treatments (Fig. 4B). In the well-watered roots, anisotropy increased gradually with position until about 5 mm from the apex and then increased steeply to a pronounced max-

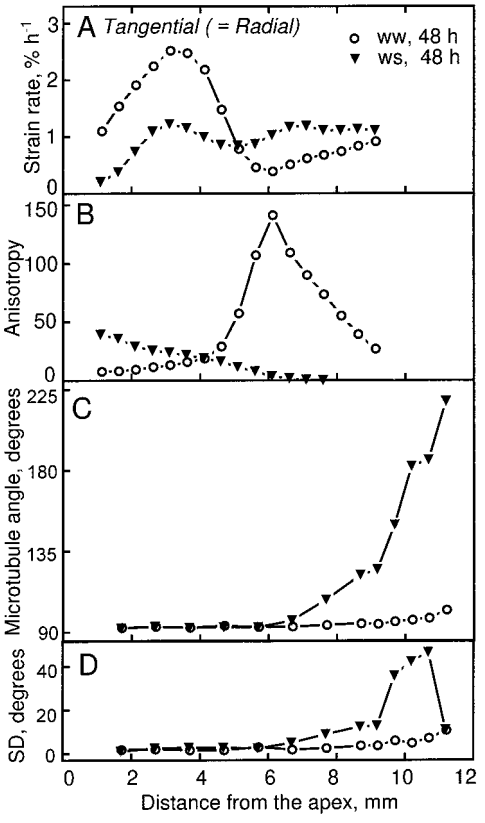

Figure 4. Tangential (radial) strain rate, growth anisotropy, and microtubule orientation as a function of distance from the apex for the stele of well-watered (ww) and water-stressed (ws) roots. A, Tangential strain rate. B, Growth anisotropy, calculated as the ratio of longitudinal to tangential strain rates. Note that the longitudinal strain rate profile shown in Figure 1A is the same for all tissues. C, Mean microtubule angle measured is stelar parenchyma. D, The SDs of the above distributions. Data in A and B are from Liang et al. (1997) and in C and D are averages of at least 100 microtubules measured per position from 5 to 10 roots.

imum, whereas in the water-stressed roots anisotropy steadily decreased with position. Microtubules in stelar parenchyma were transverse to even more basal positions than in the cortex (Fig. 4C), and as in the cortex the standard deviation of microtubule alignment increased only as microtubules became oblique (Fig. 4D). In the first 6 mm of the root, the deviations were indistinguishable between the treatments, despite the large differences in tangential strain rate and in the degree of anisotropy.

To compare clearly the onset of microtubule reorientation with the decrease in longitudinal strain rate, Figure 5 re-plots mean microtubule angle against time from the maximal longitudinal strain rate (for the well-watered treatment, only the 24-h cortical data are shown for clarity). In the cortical cells of both the well-watered and water-stressed roots, microtubules began to reorient 2 h after the peak, when the strain rates had already decreased by about 25% (Fig. 1A, arrows). In the stele the reorientation was even later, occurring about 5 h past the peak longitudinal strain rate for water-stressed roots, when the rate had nearly reached 0. (The reorientation in the stele was not defined for the well-watered roots because microtubule preservation was unreliable beyond about 12 mm from the apex.)

Assessment of Microtubule Stability

Results thus far have shown that the profiles of expansion rate were not associated with differences in microtubule orientation; however, it is possible that the profiles were associated with differential microtubule stability. To determine whether microtubules at different positions or in different treatments differed in stability, we fixed roots after first exposing them to 0°C for 3, 6, or 10 min. Cold destabilizes microtubules and will lead to their depolymerization unless they are stabilized by associated proteins (Bokros et al., 1996). Figure 6 shows that exposure for 6 min substantially depolymerized microtubules (compare with Fig. 2), but no difference was detected between treatments or positions. After a 10-min exposure, very few microtubules remained (not shown). Although subtle differences in stability would have been missed, these results suggest that there is not a large population of microtubules with significantly altered stability, either as a function of treatment or as a function of the type of orientation (i.e. transverse, helical, or longitudinal).

Quantification of Cellulose Microfibril Orientation

To quantify the orientation of microfibrils throughout the thickness of the wall, we used polarized-light microscopy to quantify the birefringent retardation of the cell wall. In the cortex the retardation of longitudinal-radial cell walls of well-watered roots at both times was approximately constant with position (Fig. 7). There was no suggestion of increased retardation around 3 mm from the apex in the 24-h treatment that might have accounted for the greatly lowered radial expansion rate at that location

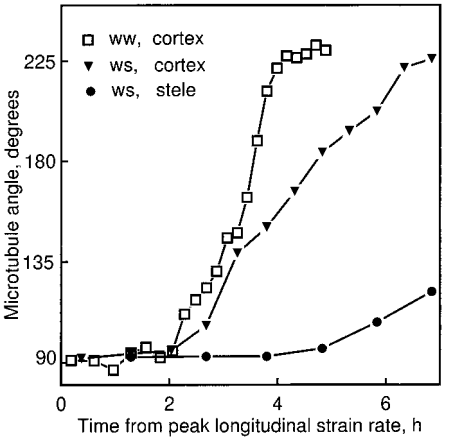

Figure 5. Mean microtubule angle as a function of time from peak longitudinal strain rate. Mean microtubule angle for the cortex of well-watered (24 h) and water-stressed (48 h) roots and for the stele of the water-stressed roots were re-plotted versus time instead of position, taking advantage of the steady-state elongation kinetics and using the transformation method described by Silk et al. (1984).

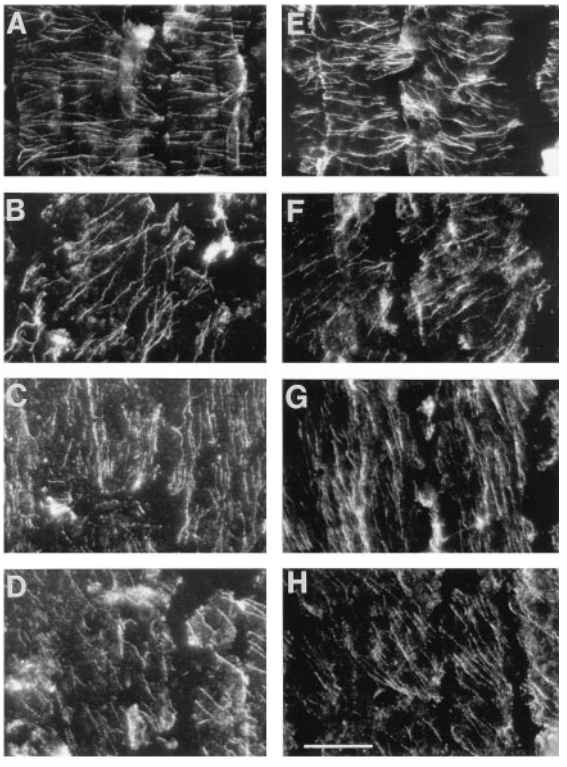

Figure 6. Micrographs showing that exposure of the seedlings to 0°C for 6 min depolymerized cortical microtubules to the same extent for transverse, oblique, and longitudinal orientations in well-watered and water-stressed roots. A to D, Well-watered roots; E to H, water-stressed roots. Examples of transverse (A and E), oblique (B and F; right-handed helical), longitudinal (C and G), and oblique (D and H; left-handed helical) microtubule orientations. Bar = 20 μm.

(and the concomitantly increased growth anisotropy). Polarized-light data were not obtained from more basal locations because adjoining walls may contain microfibrils with opposite oblique orientations (see below), which would complicate interpretation of the data. Comparing well-watered to water-stressed roots (at 48 h) showed that water stress decreased retardation of the cell walls considerably (Fig. 7), despite the fact that throughout most of this region in water-stressed roots the radial expansion rate was decreased and expansion was more anisotropic. In other words, the walls of well-watered compared with water-stressed roots expanded faster in the radial direction and less anisotropically, and yet these walls had either more cellulose per unit area of cell wall or more highly aligned cellulose (or both).

Because evidence suggests that only the inner layers of the cell wall are load-bearing (Richmond, 1983; Taiz, 1984), we also quantified the alignment of microfibrils in the innermost layers. Median longitudinal sections were extracted gently to minimize the potential for disrupting microfibrils and to ensure that images represented mainly the most recently deposited layer, and metal-carbon replicas were made and examined with electron microscopy. Figure 8 shows a representative image of a cortical cell, in which microfibrils are clearly resolved. Because of the difficulty of this method, well-watered roots were analyzed at only a single time, 24 h. Mean microfibril angle was transverse for the first 8 mm from the apex in well-watered roots and for the first 5 mm in water-stressed roots, as would be expected if microfibril orientation controlled the direction of maximal expansion rate (Fig. 9A). Basal of these positions, the mean microfibril angle became oblique, and strikingly, the sense of the obliquity differed between the treatments. As microfibrils became oblique, the direction of maximal expansion rate did not change, presumably because cells passed through this region rapidly and stopped growing before synthesizing enough oblique microfibrils to alter the direction of maximal expansion.

The standard deviation of microfibril angle was correlated with neither the observed patterns of radial expansion rate nor the degree of growth anisotropy (Fig. 9B). For example, for the well-watered roots, the deviation was virtually constant for the first 8 mm despite the differences in radial expansion rate and the degree of anisotropy (Fig. 1, B and C). Results of both methods for examining cellulose orientation concur in showing that the degree of orientation among microfibrils was correlated with neither the amount of radial expansion nor with the degree of growth anisotropy.

Relationship between Orientations of Microtubules and Microfibrils

For the diffuse growing cells of higher plants, the orientation of microtubules is widely believed to control the orientation of microfibrils. Our results are fully consistent with this belief where these elements were transverse. However, for the water-stressed roots, comparison of Figures 3 and 9 shows that microtubules reoriented to oblique angles greater than 90° (right-handed helices) but microfibrils reoriented to angles less than 90° (left-handed helices). To ensure that this was not a sampling discrepancy between the different experiments, we modified our proce-

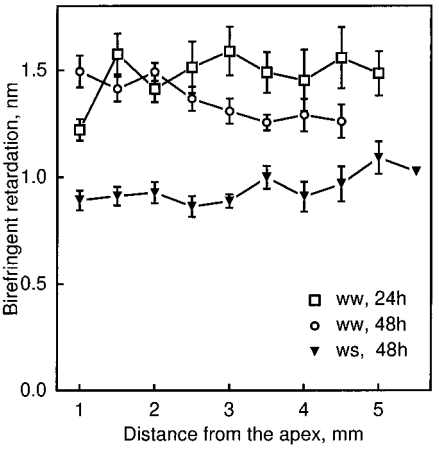

Figure 7. Birefringent retardation as a function of distance from the apex of well-watered (ww) and water-stressed (ws) roots. Cortical cell walls were measured in approximately median-longitudinal sections in 2-μm semithin methacrylate sections. Data are means ± SE of five roots, with two cell walls sampled at each position per section and three sections measured per root.

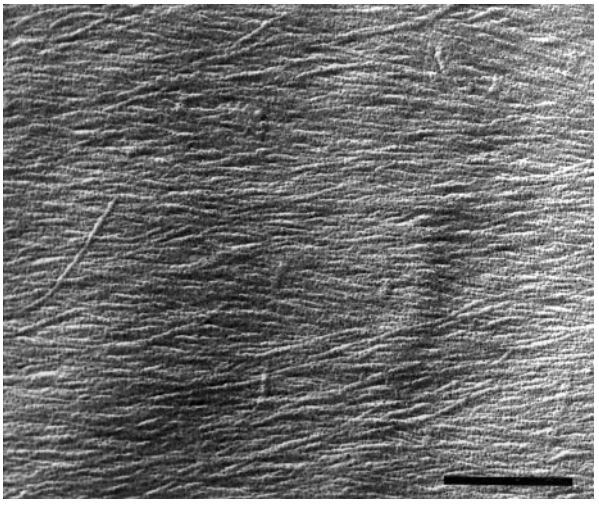

Figure 8. Electron micrograph showing the appearance of microfibrils on the innermost layer of a longitudinal-radial cell wall of a cortical cell from a well-watered root. Image shows a cell with a net transverse orientation of microfibrils, approximately 5 mm from the apex. The longitudinal axis of the root is parallel to the side of the figure. Vibratome sections were extracted with carbonate and a metal-carbon replica was made as described in "Materials and Methods." Bar = 400 nm.

dures so that microtubules and microfibrils could be examined in the same section. For this analysis, we counted the number of cells having orientations judged visually to be in one of the following classes: undefined, transverse, right-handed helical, longitudinal, and left-handed helical. The orientations of microtubules and microfibrils of water-stressed roots are compared in Figure 10 by showing the frequency of cells with a given class of orientation at four positions. The orientation of microtubules went from predominantly right-handed helical at 6 mm, through longitudinal, to predominantly left-handed helical. However, cellulose microfibrils at 6 and 7 mm from the apex occurred in both helical forms about equally and then became predominantly right-handed helical, which was opposite to the prevalent orientation of the microtubules.

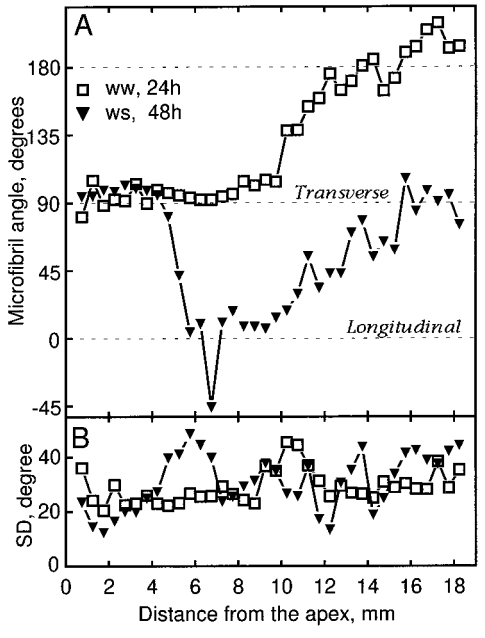

Figure 9. Microfibril orientation as a function of distance from the apex of well-watered (ww) and water-stressed (ws) roots. A, Mean microfibril angle measured for cortical cells in longitudinal sections. B, The SDs of the above distributions. Data are averages of 250 to 1800 microfibrils measured per position from three experiments with five roots each.

DISCUSSION

To understand how the degree of anisotropic expansion is controlled, we have studied how the shape of the maize primary root changes developmentally and in response to water stress. To our knowledge, this is the only study to have quantified growth anisotropy in different tissues as well as orientations of microtubules and microfibrils in the same material. Our results are consistent with the prevalent view that the direction of maximal expansion rate is specified by the mean orientation of microtubules and microfibrils; however, we also show that changes in the degree of growth anisotropy are apparently not specified by the orientation of either microtubules or microfibrils.

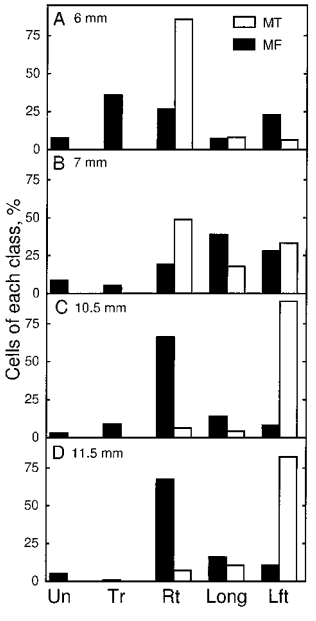

Figure 10. In water-stressed roots the handedness of helical orientations of microfibrils is in many cells opposite to that of the microtubules. Percentage of cortical cells with various classes of orientations of microtubules (MT, white bars) and microfibrils (MF, black bars) at 6 mm (A), 7 mm (B), 10.5 mm (C), and 11.5 mm (D) from the apex are shown. Percentages of cells with undefined (Un), transverse (Tr), right-handed helical (Rt), longitudinal (Long), and left-handed helical (Lft) orientations are also shown. Orientations of each element were measured in the same sections. Data for microtubules are means of 100 to 140 cells, and for microfibrils of 270 to 560 cells, from single median-longitudinal sections from five to seven roots.

Orientation and Stability of Cortical Microtubules

Cortical microtubule arrays are well known to change their mean orientation in response to various stimuli (Williamson, 1991), but intermediate stages in the reorientation have rarely been observed. We found that mean microtubule orientation changed steadily at an average rate of 1° min^{-1} in well-watered roots and more slowly in water-stressed roots. In pea epidermis, although it took about 45 min for the mean microtubule orientation to rotate through 45° (i.e. similar to the rate seen here), the reorientation was discontinuous in each cell, with groups of microtubules reorienting sooner than others (Wymer and Lloyd, 1996). In contrast, microtubule orientation in both the stele and cortex of the maize root remained highly uniform until becoming longitudinal, when the standard deviation for microtubule angle increased abruptly (Fig. 3B). Our results are consistent with both leading models for the mechanism of reorientation (Cyr, 1994; Hepler and Hush, 1996; Wymer and Lloyd, 1996) involving either physical rotation or selective stabilization of microtubules.

Our results showing that microtubule arrays of different orientations and in the different treatments had a uniform sensitivity to cold differ from previous reports. Baluška et al. (1993) reported that the cold stability of microtubules in the maize root differed as a function of position. For pea epidermis, transversely oriented microtubules were reported to be more cold-labile than longitudinal ones (Akashi and Shibaoka, 1987). Also, in the same material, longitudinal orientation and cold stability were both promoted by abscisic acid (Sakiyama and Shibaoka, 1990). The latter finding is relevant to this study because in the water-stressed maize root abscisic acid accumulates, reaching 5 to 10 times the well-watered levels in the apical 5 mm of the root (Saab et al., 1992). The uniform response of microtubules to cold reported here, in contrast to the divergent responses reported elsewhere, might be explained by the use of different organs, species, or cultivars; alternatively, the explanation might be the duration of cold treatment, which was 10 min or less here but 1 h or more in the other studies. The half-life of cortical microtubules is short, approximately 1 min (Hepler and Hush, 1996); therefore, a treatment that blocks microtubule polymerization should remove more than 99% of the cortical array by 10 min. After 1 h or more of cold, cells will have begun to acclimate, which has been shown to include synthesis of cold-tolerant tubulin isotypes (Chu et al., 1993). Therefore, microtubule arrays present after 1 h or more of cold probably reflect acclimation rather than microtubule dynamics at the onset of the cold treatment.

Orientation of Cellulose Microfibrils: Polarized-Light and Electron Microscopy

To assess microfibril orientation, we used both polarized-light and electron microscopy of replicas of the innermost surface of the wall. In recent years studies of the structure of primary cell walls and its relation to growth have focused on the innermost cell wall layer, as revealed by electron microscopy, because it is now widely believed that only the innermost layers of the cell wall are load-bearing. This view arose from studies of the giant internodal cells of characean algae, for which evidence was obtained that only the inner 25% of cell wall controlled the directional yielding behavior of the cell (Richmond, 1983; Taiz, 1984). Since 25% of the wall of these extraordinary cells exceeds by many times the thickness of most primary walls of higher plants, the proportion of load-bearing cell wall thickness in the internodes may not scale to thinner cell walls. Therefore, the mechanical reinforcement of a primary higher plant cell wall may extend throughout most, if not all, of its thickness.

For a cell wall, the amount of retardation reflects the amount of crystalline microfibrils in the light path, as well as their average degree of orientation (Preston, 1974). Retardation of cell walls of water-stressed roots was less than that of the well-watered roots, whereas microfibril alignment at the innermost layer of the two treatments had about the same variability. This could be explained by microfibrils reorienting after deposition as a result of being rotated passively by the expansion of the cell wall, because the amount of this rotation is predicted to be proportional to the degree of growth anisotropy (Erickson, 1980; Preston, 1982). The greater anisotropy in the apical portion of the water-stressed roots would be expected to rotate microfibrils farther away from transverse and, consequently, to decrease retardation, as was observed. However, the predicted extent of the rotation is modest for the majority of microfibrils, and it is doubtful that the predicted difference in rotation would amount to a detectable signal. On the other hand, the lesser retardation could be explained by cell walls of the water-stressed roots having fewer microfibrils per unit area, which would result if water stress had decreased cellulose synthesis. Regardless of whether the lesser retardation in the water-stressed cortical cell walls resulted from a decrease in cellulose synthesis or from more passive rotation of microfibrils, less retardation was hypothesized to make growth less anisotropic, which is the opposite of what occurred.

Microtubule-Microfibril Parallelism

In studies of microtubule and microfibril parallelism, most researchers have compared mean orientations and only a few have compared the variability of alignment. We found that microtubules were more highly aligned than the microfibrils, as judged by the much smaller standard deviations of their angular distribution (Fig. 3B versus Fig. 9B). In contrast, Sassen and Wolters-Arts (1986) reported that in stamen hairs of *Tradescantia virginiana* angular distributions of microtubules were either about the same or larger than those of the microfibrils (measured in replicas), and Seagull (1992) reported that in cotton hairs the degree of variability of microtubules was nearly identical to that of the microfibrils (in replicas); the variability of both decreased in parallel from nearly random in young hairs to extremely well aligned in nongrowing hairs. It is possible that we underestimated the variability of microtubule orientation through imaging microtubules with light microscopy, because the diameter of a microtubule is 10 times less

than the limit of resolution (Williamson, 1991). Nevertheless, it is unlikely that this effect could account entirely for the better alignment of the microtubules. The alignment of microtubules has been hypothesized to affect the alignment of microfibrils by direct or indirect mechanisms (Emons et al., 1992; Wymer and Lloyd, 1996). For the maize root, our results suggest that if microfibril deposition is coupled to microtubules directly, e.g. by a motor protein, then the coupling must be transient to allow for the greater divergence among microfibrils.

In addition to the systematic difference in the variability of alignments of microtubules and microfibrils, we also found a striking difference in their mean orientation. The orientations of microtubules and microfibrils were parallel where these elements were both transverse, but the alignments diverged when they became helical. This was obvious for the water-stressed roots in which the mean orientations of microtubules and microfibrils indicated helices of opposite handedness, but was also true for the well-watered roots in regions of helical orientation. For example, in well-watered roots between 12 and 18 mm from the apex, mean microfibril angle was approximately 180°, whereas mean microtubule angle was 225°. Moreover, analysis of different classes of orientation (as reported for water-stressed roots in Fig. 10) revealed many cells with left- and right-handed helical microfibril orientation at the same position (data not shown). In contrast, the orientation of helical microtubule arrays at a given position was strictly uniform (Liang et al., 1996). Thus, in both treatments, where microtubules were helical, microfibrils were not always co-aligned. In pea roots mean orientations of microtubules and microfibrils have been found to be parallel (Hogetsu, 1986; Hogetsu and Oshima, 1986), but it was not determined whether oblique orientations reflected helices of similar or opposite handedness. Similar to our findings, in roots of onion and radish microtubules paralleled microfibrils when both were transverse, but were not always parallel when mean orientations were helical (Traas and Derksen, 1989).

Opposite helical alignment contradicts the prevalent view of microtubules aligning microfibrils. A helical alignment of microfibrils may represent a default orientation state that can form independently of microtubules (Emons, 1994). In some cell types microfibrils are known to be deposited helically without requiring microtubules, as in root hairs (Emons et al., 1992) and in some green algae (Mizuta et al., 1989; Kimura and Mizuta, 1994). Most evidence supporting a role for microtubules in the alignment of microfibrils suggests that microtubules are required for coherent organization of cellulose throughout a cell or tissue but not for the local organization of microfibrils in single cells or regions of cells. Thus, when microtubules are depolymerized, there are only a few examples in which the alignment of microfibrils becomes random (Hogetsu and Shibaoka, 1978), but many in which microfibrils remain well aligned locally but lose the consistency of alignment across the cell or tissue (Itoh, 1976; Takeda and Shibaoka, 1981; Mueller and Brown, 1982). In the maize root it is possible that the transverse deposition of microfibrils requires the presence of transverse microtubules but that, as microtubule organization becomes helical, microfibril deposition becomes uncoupled from microtubules and assumes a helical pattern by virtue of some other organizing influence.

Growth Anisotropy and the Role of the Epidermis

Our results bear on how microtubules and microfibrils may control elongation rates as well as rates of radial and tangential expansion. We found that microtubules and microfibrils reoriented from transverse to oblique after elongation rate had already declined significantly, and we found that the degree of alignment among microtubules and microfibrils did not explain rates of radial expansion or the degree of anisotropy. Both of these conclusions might be argued against because we did not examine the epidermis. The epidermis is believed to exert a dominant influence on the elongation of shoots (Kutschera, 1992), and in the maize root, the outer epidermal wall includes a thick pellicle in the apical 4 to 5 mm of the root and resembles ultrastructurally the outer epidermal cell wall of the shoot (Abeysekera and McCully, 1993a). However, that the epidermis limits elongation rates in roots is doubtful. Björkman and Cleland (1991) removed the epidermis from maize roots and found that the spatial profile of longitudinal strain rate was unaffected.

The epidermis is even less likely to play a role in limiting radial or tangential expansion. Despite the shoot epidermis having been investigated intensively with respect to elongation, to our knowledge, its role in controlling radial and tangential expansion has never been studied. Because different tissues expand radially at different rates, as seen here for the cortex and stele (Figs. 1B and 4A), these rates cannot be limited by a single tissue. Moreover, when the stele expands radially but the cortex does not (as seen here around 3 mm from the tip), the cortex and the epidermis must nevertheless expand tangentially or be split by the expanding stele. Thus, at least in the tangential direction, outer tissues need to be compliant to the radial or tangential expansion of inner tissues. In agreement with this, it has been reported for maize roots that the excised outer epidermal wall is highly compliant tangentially (Abeysekera and McCully, 1994). Finally, further doubt is cast on the root epidermis limiting radial or tangential expansion by genetic evidence. In *Arabidopsis thaliana* (Baskin et al., 1992) and maize (Abeysekera and McCully, 1993b), mutants have been characterized in which cells of the root epidermis are swollen or distorted, and in the maize mutant the thick epidermal pellicle is nearly absent; however, except for the distorted epidermis, the roots of the mutants have the same diameter as those of the wild type.

Microtubules, Microfibrils, and the Control of Growth Anisotropy

We have found that the orientations of microtubules and microfibrils change predictably during development, from transverse in rapidly expanding cells to helical in nongrowing cells. A similar developmental sequence for the alignments of these elements has been reported for various plant

organs, including roots (Hogetsu, 1986; Hogetsu and Oshima, 1986). However, from previous reports one could not determine whether the reorientation of microtubules and microfibrils preceded or followed the decrease in elongation rate because the spatial profile of elongation rate was not measured with sufficient accuracy. In contrast, Pritchard et al. (1993) measured elongation of the maize root with enough spatial accuracy but measured microfibril angles at only four locations. Our results show that as cells moved through the growth zone, the reorientation of microtubules and microfibrils followed the decrease in elongation rate by 2 h in the cortex and by even longer in the stele. Evidently, the developmental changes in the orientations of microtubules and microfibrils do not cause the changes in the rate of elongation.

Concerning radial and tangential expansion, we undertook this investigation to learn how the degree of expansion anisotropy is controlled. We hypothesized that this control is exerted by the degree of alignment among cellulose microfibrils. This is an economical hypothesis in that microfibrils would control the direction of maximal expansion through their mean orientation, as well as the degree of anisotropy through the dispersion around the mean orientation. This hypothesis was first made by Green (1964), who compared two algae, *Nitella axillaris* and *Hydrodictyon africanum*, and found that the greater degree of growth anisotropy in *N. axillaris* was associated with more highly aligned microfibrils. Although Green's data may indicate that the hypothesis is sometimes true, instead they may reflect fortuitous differences in wall structure between the two divergent algal species. Also consistent with the hypothesis, Probine (1965) found that as the diameter of excised pea epicotyls increased in the presence of increasing concentrations of cytokinin, regions of the cell wall with transverse microfibrillar orientation had decreased retardation. However, the increased diameter may have been caused instead by bands of longitudinal microfibrils that appeared in hormone-treated material and increased in prominence with concentration. For the maize root, we falsified the hypothesis by finding that changes in the degree of growth anisotropy were accompanied by a constant degree of alignment among microfibrils, both throughout the cell wall and at the innermost layer.

If the degree of expansion anisotropy is not controlled by the degree of alignment among microfibrils, then what does exert this control? We hypothesize that cell wall yielding is regulated independently in longitudinal and radial directions. Such independent regulation would occur if longitudinal extensibility were regulated by specific cell wall components that resist the separation of microfibrils, whereas radial extensibility would be regulated by other components that resist shear between microfibrils. Considerable evidence suggests that elongation is limited at least to some extent by the network of hemicellulose that enmeshes microfibrils (Cosgrove, 1997). However, as Liang et al. (1997) pointed out, for the treatments studied here, the activities of two enzymes, expansin and xyloglucan endotransglycosylase, thought to loosen this network, are correlated with longitudinal strain rates but not with radial or tangential strain rates. Although cell wall components that are active radially have not been identified biochemically, they may have been identified genetically. Tsuge et al. (1996) identified two loci in *A. thaliana* that exert independent control of expansion in length and width of leaves. Two other *A. thaliana* loci have been identified that are required for highly anisotropic growth in roots not for the transverse orientation of microtubules or microfibrils (A. Wiedemeier, T.I. Baskin, unpublished data). Possibly, such loci encode activities that regulate the ability of aligned microfibrils to resist shear stress.

Our results show that in higher plants, unlike in the *N. axillaris* internode, the degree of growth anisotropy varies, and this variation produces adaptive changes in organ shape, such as the thinning of roots in response to water stress. The extent of growth anisotropy has been neglected by models relating cell wall architecture to expansion, which have dealt solely with elongation (Cosgrove, 1997). These models must be extended to encompass the full three-dimensional yielding behavior of the cell wall before plant morphogenesis can be fully understood.

ACKNOWLEDGMENTS

We thank Jan Wilson for flawless technical assistance and Corine van der Weele for thoughtful comments on the manuscript.

Received July 22, 1998; accepted November 7, 1998.

LITERATURE CITED

Abeysekera RM, McCully M (1993a) The epidermal surface of the maize root tip. I. Development in normal roots. New Phytol **125:** 413–430

Abeysekera RM, McCully M (1993b) The epidermal surface of the maize root tip. II. Abnormalities in a mutant which grows crookedly through soil. New Phytol **125:** 801–811

Abeysekera RM, McCully M (1994) The epidermal surface of the maize root tip. III. Isolation of the surface and characterization of some of its structural and mechanical properties. New Phytol **127:** 321–333

Akashi T, Shibaoka H (1987) Effects of gibberellin on the arrangement and the cold stability of cortical microtubules in epidermal cells of pea internodes. Plant Cell Physiol **28:** 339–348

Arioli T, Peng L, Betzner AS, Burn J, Wittke W, Herth W, Camilleri C, Höfte H, Plazinski J, Birch R, and others (1998) Molecular analysis of cellulose biosynthesis in Arabidopsis. Science **179:** 717–720

Baluška F, Parker JS, Barlow PW (1993) The microtubular cytoskeleton in cells of cold-treated roots of maize (*Zea mays* L.) shows tissue-specific responses. Protoplasma **172:** 84–96

Baskin TI, Betzner AS, Hoggart R, Cork A, Williamson RE (1992) Root morphology mutants in *Arabidopsis thaliana*. Aust J Plant Physiol **19:** 427–437

Baskin TI, Wilson JE (1997) Inhibitors of protein kinases and phosphatases alter root morphology and disorganize cortical microtubules. Plant Physiol **113:** 493–502

Bayley ST, Colvin JR, Cooper FP, Martin-Smith CA (1957) The structure of the primary epidermal cell wall of *Avena* coleoptiles. J Biophys Biochem Cytol **3:** 171–182

Björkman T, Cleland RE (1991) Root growth regulation and gravitropism in maize roots does not require the epidermis. Planta **185:** 34–37

Bokros CL, Hugdahl JD, Blumenthal SD, Morejohn C (1996) Proteolytic analysis of polymerized maize tubulin: regulation of microtubule stability to low temperature and Ca^{2+} by the carboxyl terminus of β-tubulin. Plant Cell Environ **19:** 539–548

Brown RM Jr, Saxena IM, Kudlicka K (1996) Cellulose biosynthesis in higher plants. Trends Plant Sci **1:** 149–156

Carlemalm E, Garavito RM, Villiger W (1982) Resin development for electron microscopy and an analysis of embedding at low temperature. J Microsc **126:** 123–143

Castle ES (1958) The topography of tip growth in a plant cell. J Gen Physiol **41:** 913–926

Chu B, Snustad DP, Carter JV (1993) Alteration of β-tubulin gene expression during low-temperature exposure in leaves of *Arabidopsis thaliana*. Plant Physiol **103:** 371–377

Cosgrove DJ (1997) Relaxation in a high-stress environment: The molecular bases of extensible cell walls and cell enlargement. Plant Cell **9:** 1031–1041

Cyr RJ (1994) Microtubules in plant morphogenesis: role of the cortical array. Annu Rev Cell Biol **10:** 153–180

Emons AMC (1994) Winding threads around plant cells: a geometrical model for microfibril deposition. Plant Cell Environ **17:** 3–14

Emons AMC, Derksen J, Sassen MMA (1992) Do microtubules orient plant cell wall microfibrils? Physiol Plant **84:** 486–493

Erickson RO (1980) Microfibrillar structure of growing plant cell walls. *In* WM Getz, ed, Mathematical Modelling in Biology and Ecology, Lecture Notes in Biomathematics, Vol 33. Springer-Verlag, Berlin, pp 192–212

Green PB (1964) Cell walls and the geometry of plant growth. Brookhaven Symp Biol **16:** 203–217

Green PB (1965) Pathways of cellular morphogenesis. A diversity in *Nitella*. J Cell Biol **27:** 343–363

Green PB (1980) Organogenesis—a biophysical view. Annu Rev Plant Physiol **31:** 51–82

Hepler PK, Hush JM (1996) Behavior of microtubules in living plant cells. Plant Physiol **112:** 455–461

Hogetsu T (1986) Orientation of wall microfibril deposition in root cells of *Pisum sativum* L. var. Alaska. Plant Cell Physiol **27:** 947–951

Hogetsu T (1989) The arrangement of microtubules in leaves of monocotyledonous and dicotyledonous plants. Can J Bot **67:** 3506–3512

Hogetsu T, Oshima Y (1986) Immunofluorescence microscopy of microtubule arrangement in root cells of *Pisum sativum* L. var Alaska. Plant Cell Physiol **27:** 939–945

Hogetsu T, Shibaoka H (1978) Effects of colchicine on cell shape and on microfibril arrangement in the cell wall of *Closterium acerosum*. Planta **140:** 15–18

Hogetsu T, Shibaoka H, Shimokoriyama M (1974) Involvement of cellulose synthesis in actions of gibberellin and kinetin on cell expansion. Gibberellin-coumarin and kinetin-coumarin interactions on stem elongation. Plant Cell Physiol **15:** 265–272

Itoh T (1976) Microfibrillar orientation of radially enlarged cells of coumarin- and colchicine-treated pine seedlings. Plant Cell Physiol **17:** 385–398

Iwata K, Hogetsu T (1989) Orientation of wall microfibrils in *Avena* coleoptiles and mesocotyls and in *Pisum* epicotyls. Plant Cell Physiol **30:** 749–757

Jerrard HG (1948) Optical compensators for measurement of elliptical polarization. J Optical Soc Am **38:** 35–59

Kimura S, Mizuta S (1994) Role of the microtubule cytoskeleton in alternating changes in cellulose microfibril orientation in the coenocytic green alga, *Chaetomorpha moniligera*. Planta **193:** 21–31

Kutschera U (1992) The role of the epidermis in the control of elongation growth in stems and coleoptiles. Bot Acta **105:** 246–252

Liang BM, Dennings AM, Sharp RE, Baskin TI (1996) Consistent handedness of microtubule helical arrays in maize and Arabidopsis primary roots. Protoplasma **190:** 8–15

Liang BM, Sharp RE, Baskin TI (1997) Regulation of growth anisotropy in well-watered and water-stressed maize roots. I. Spatial distribution of longitudinal, radial and tangential expansion rates. Plant Physiol **115:** 101–111

Mizuta S, Kurogi U, Okuda K, Brown RM Jr (1989) Microfibrillar structure, cortical microtubule arrangement and the effect of amiprophos-methyl on microfibril orientation in the thallus cells of the filamentous green alga, *Chamaedoris orientalis*. Ann Bot **64:** 383–394

Mueller SC, Brown RM Jr (1982) The control of cellulose microfibril deposition in the cell wall of higher plants. II. Freeze-fracture microfibril patterns in maize seedling tissues following experimental alteration with colchicine and ethylene. Planta **154:** 501–515

Preston RD (1974) The Physical Biology of Plant Cell Walls. Chapman & Hall, London

Preston RD (1982) The case for multinet growth in growing walls of plant cells. Planta **155:** 356–363

Pritchard J, Hetherington PR, Fry SC, Tomos AD (1993) Xyloglucan endotransglycosylase activity, microfibril orientation and the profiles of cell wall properties along growing regions of maize roots. J Exp Bot **44:** 1281–1289

Probine MC (1965) Chemical control of plant cell wall structure and of cell shape. Proc R Soc Lond B Biol Sci **161:** 526–537

Richmond PA (1983) Patterns of cellulose microfibril deposition and rearrangement in *Nitella*: in vivo analysis by a birefringence index. J Appl Polymer Sci Appl Polymer Symp **37:** 107–122

Saab IN, Sharp RE, Pritchard J (1992) Effect of inhibition of abscisic acid accumulation on the spatial distribution of elongation in the primary root and mesocotyl of maize at low water potentials. Plant Physiol **99:** 26–33

Sakaguchi S, Hogetsu T, Hara N (1990) Specific arrangements of cortical microtubules are correlated with the architecture of meristems in shoot apices of angiosperms and gymnosperms. Bot Mag Tokyo **103:** 143–163

Sakiyama M, Shibaoka H (1990) Effects of abscisic acid on the orientation and cold stability of cortical microtubules in epicotyl cells of the dwarf pea. Protoplasma **157:** 165–171

Sassen MMA, Wolters-Arts AMC (1986) Cell wall texture and cortical microtubules in growing staminal hairs of *Tradescantia virginiana*. Acta Bot Neerl **35:** 351–360

Seagull RW (1992) A quantitative electron microscopic study of changes in microtubule arrays and wall microfibril orientation during in vitro cotton fiber development. J Cell Sci **101:** 561–577

Sharp RE, Hsiao TC, Silk WK (1990) Growth of the maize primary root at low water potentials. II. Role of growth and deposition of hexose and potassium in osmotic adjustment. Plant Physiol **93:** 1337–1346

Sharp RE, Silk WK, Hsiao TC (1988) Growth of the maize primary root at low water potentials. I. Spatial distribution of expansive growth. Plant Physiol **87:** 50–57

Shedletzky E, Shmuel M, Delmer DP, Lamport DTA (1990) Adaptation and growth of tomato cells on the herbicide 2, 6-dichlorobenzonitrile leads to production of unique cell walls virtually lacking a cellulose-xyloglucan network. Plant Physiol **94:** 980–987

Silk WK, Abou Haidar S (1986) Growth of the stem of *Pharbitis nil*: analysis of longitudinal and radial components. Physiol Veg **24:** 109–116

Silk WK, Walker RC, Labavitch J (1984) Uronide deposition rates in the primary root of *Zea mays*. Plant Physiol **74:** 721–726

Taiz L (1984) Plant cell expansion: regulation of cell wall mechanical properties. Annu Rev Plant Physiol **35:** 585–657

Takeda K, Shibaoka H (1981) Effects of gibberellin and colchicine on microfibril arrangement in epidermal cell walls of *Vigna angularis* Ohwi et Ohashi epicotyls. Planta **151:** 393–398

Traas JA, Derksen J (1989) Microtubules and cellulose microfibrils in plant cells: simultaneous demonstration in dry cleave preparations. Eur J Cell Biol **48:** 159–164

Tsuge T, Tsukaya H, Uchimiya H (1996) Two independent and polarized processes of cell elongation regulate leaf blade expansion in *Arabidopsis thaliana* (L.) Heynh. Development **122:** 1589–1600

Williamson RE (1991) Orientation of cortical microtubules in interphase plant cells. Int Rev Cytol **129:** 135–206

Wymer C, Lloyd C (1996) Dynamic microtubules: implications for cell wall patterns. Trends Plant Sci **1:** 222–228